Electrical transport and magnetic properties of La$_{0.5}$Ca$_{0.5}$MnO$_{3-y}$ with varying oxygen content

Y. G. Zhao,[1,2,*] W. Cai,[1] J. Zhao,[1] X. P. Zhang,[1] B. S. Cao,[1,2] M. H. Zhu,[1] L. W. Zhang,[1] S. B. Ogale,[3] Tom Wu,[3] T. Venkatesan,[3] Li Lu,[4] T. K. Mandal,[5] and J. Gopalakrishnan[5]

[1]Department of Physics, Tsinghua University, Beijing 100084, People's Republic of China
[2]School of Materials Science and Engineering, Tsinghua University, Beijing 100084, People's Republic of China
[3]Center for Superconductivity Research, Department of Physics, University of Maryland, College Park, Maryland 20742
[4]Institute of Physics, Chinese Academy of Sciences, Beijing 100080, People's Republic of China
[5]Solid State and Structural Chemistry Unit, Indian Institute of Science, Bangalore 560 012, India

We report the tuning of oxygen content of La$_{0.5}$Ca$_{0.5}$MnO$_{3-y}$ and its effect on electrical transport and magnetic properties. A small reduction of oxygen content leads to a decrease in sample resistivity, which is more dramatic at low temperatures. No significant change is seen to occur in the magnetic properties for this case. Further reduction in the oxygen content increases the resistivity remarkably, as compared to the as-prepared sample. The amplitude of the ferromagnetic (FM) transition at 225 K decreases, and the antiferromagnetic (AFM) transition at 130 K disappears. For samples with $y=0.17$, insulator-metal transition and paramagnetic-ferromagnetic transition occur around 167 K. The results are explained in terms of the effect of oxygen vacancies on the coexistence of the metallic FM phase and the insulating charge ordered AFM phase.

PACS number(s): 75.50.Dd; 72.80.Ga

INTRODUCTION

The hole doped rare-earth manganites $L_{1-x}A_x$MnO$_3$, where L and A are trivalent lanthanide and divalent alkaline-earth ions, have become the subject of intense research because of their importance for both fundamental issues in condensed-matter physics and the potential for applications.[1–4] It has been shown that spin, charge, and lattice are strongly coupled in these compounds[5–7] leading to various properties in the phase diagram of $L_{1-x}A_x$MnO$_3$.[8] One of the most interesting features encountered in the phase diagram for the ground state of La$_{1-x}$Ca$_x$MnO$_3$ is the change from ferromagnetic (FM) to charge ordering antiferromagnetic (AFM) insulator when the Ca doping amount crosses 0.5.[8] Clearly, the phase boundary compound La$_{0.5}$Ca$_{0.5}$MnO$_3$ is very unique, and not surprisingly, is the focus of great scientific interest.[9–26] It has been shown that upon lowering temperature, this compound first undergoes a paramagnetic (PM) to FM phase transition at $T_c \approx 225$ K and then to a charge ordering AFM phase at $T_{co} \approx 155$ K.[8,10,27] The charge ordering state can be destroyed by magnetic field,[28,29] x-ray irradiation,[30] and Mn site doping with 1% Cr.[31,32] However, it is not known how robust is the charge ordered (CO) state with respect to decrease of oxygen content. Decreasing the oxygen content would increase the Mn^{3+}/Mn^{4+} ratio in the series La$_{0.5}$Ca$_{0.5}$MnO$_{3-y}$, and for $y=0.25$, the sample would have 100% Mn^{3+}. For intermediate values, $0<y<0.25$, the Mn^{3+}/Mn^{4+} ratio would vary inversely to that in La$_{1-x}$Ca$_x$MnO$_3$ as a function of x. Accordingly, in principle, one could expect to simulate the properties of the La$_{1-x}$Ca$_x$MnO$_3$ system in La$_{0.5}$Ca$_{0.5}$MnO$_{3-y}$, by changing y. Recently, it has been shown that metallic FM phase coexists with the insulating CO AFM phase in the low-temperature state of La$_{0.5}$Ca$_{0.5}$MnO$_3$ at the microscopic level.[10,11,13,15] The coexistence of these two phases originates from the small energy difference between them. Thus it is also interesting to study the effect of the oxygen content on the energy balance in the system, and thereby on the coexistence of these two phases.

In this paper, we report the electrical transport and magnetic properties of La$_{0.5}$Ca$_{0.5}$MnO$_{3-y}$ with different oxygen contents. Upon decreasing the oxygen content, the resistivity decreases, especially at lower temperatures, while the magnetic property does not show an obvious change. When further reducing the oxygen content, the resistivity of the sample increases dramatically as compared to the as-prepared sample, and the amplitude of the FM transition decreases in addition to the disappearance of the AFM transition. Insulator-metal and paramagnetic-ferromagnetic transitions were observed around 167 K in the sample with $y=0.17$. The results clearly reveal the crucial role played by oxygen content on the coexistence of the FM metallic and charge ordered AFM insulating state.

EXPERIMENT

The La$_{0.5}$Ca$_{0.5}$MnO$_3$ samples were prepared by solid state reaction method using high purity La$_2$O$_3$, CaCO$_3$, MnO$_2$ powders with appropriate atomic ratio. The mixed powder was ground and calcined at 1050 °C several times. The calcined powders were then pressed into pellets and sintered at 1300 °C for 8 h in air followed by slow cooling. In order to reduce the oxygen content of the samples, we annealed the samples in flowing N$_2$ with graphite powder placed near the samples. The oxygen contents of the samples were measured by titration method,[33] and the oxygen content was found to be reproducible within ± 0.005. The phase analysis of the samples was performed using a Rigaku D/max-RB x-ray diffractometer with Cu $k\alpha$ radiation. The electrical resistivity was measured by the four-probe method. The ac susceptibility was measured from room temperature down to 77 K. A
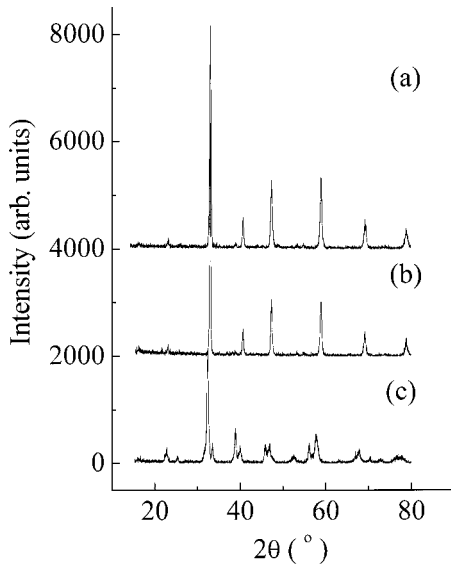
FIG. 1. X-ray-diffraction patterns of the $La_{0.5}Ca_{0.5}MnO_{3-y}$ samples of (a) as-prepared, (b) 850 °C annealed, and (c) 900 °C annealed.

superconducting quantum interference device (SQUID) magnetometer was used to measure the temperature dependence of magnetization with samples mounted in a plastic soda straw. The magnetic field was parallel to the sample surface. Both zero-field-cooling (ZFC) and field-cooling (FC) data were recorded.

RESULTS AND DISCUSSION

Figure 1 shows the x-ray-diffraction patterns of the (a) as-prepared, (b) 850 °C annealed, and (c) 900 °C annealed $La_{0.5}Ca_{0.5}MnO_{3-y}$ samples. It can be seen that the x-ray-diffraction pattern of the 850 °C annealed sample is similar to that of the as-prepared sample, indicating that no structure change occurs, although the oxygen content for the 850 °C annealed sample is reduced remarkably as shown below. However, the x-ray-diffraction pattern of the 900 °C annealed sample shows dramatic change as compared to that of the as-prepared sample, suggesting that a structure change or decomposition of $La_{0.5}Ca_{0.5}MnO_{3-y}$ occurred due to the reduction of the oxygen content. The oxygen content of the as-prepared, 800 and 850 °C annealed samples are 3.013, 2.996, and 2.785, respectively, as determined by the titration method. Therefore annealing at 800 °C does not reduce the oxygen content of the sample very much, however, annealing at 850 °C dramatically reduces the oxygen content of the sample.

Figure 2 shows the temperature dependence of resistivity for different samples. Sample A is the as-prepared $La_{0.5}Ca_{0.5}MnO_{3-y}$ sample, sample B is the sample annealed at 600 °C for 12 h in flowing N_2 with graphite powder nearby, and sample C is the sample annealed at 800 °C for 12 h in flowing N_2 with graphite powder nearby. The inset gives the temperature dependence of resistivity for the samples annealed at 800 °C (curve C) and 850 °C (curve D) for 12 h in flowing N_2 with the graphite powder nearby, respectively.
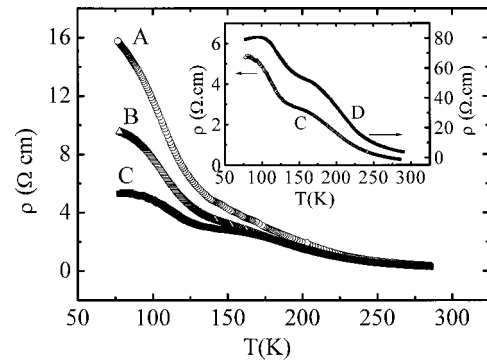
FIG. 2. Temperature dependence of resistivity for different $La_{0.5}Ca_{0.5}MnO_{3-y}$ samples. (A) as-prepared, (B) annealed at 600 °C in flowing N_2 for 12 h with the graphite powder nearby, (C) annealed at 800 °C in flowing N_2 for 12 h with the graphite powder nearby. The inset gives the temperature dependence of resistivity for samples annealed at 800 °C (curve C) and 850 °C (curve D) for 12 h in flowing N_2 with the graphite powder nearby, respectively.

Below 800 °C, the resistivity of the samples decreases with the increase of the annealing temperature, especially at low temperatures; while the resistivity for the 850 °C annealed sample increases dramatically. An upturn of resistivity is clearly observed for all the samples around 130 K, which corresponds to the charge ordering temperature. This temperature for resistivity upturn corresponds well to the temperature at which the ac susceptibility drops due to the AFM transition (Fig. 4). In Fig. 2, it can also be seen that a shoulder appears at 175 K for the annealed samples, and is prominent for the 850 °C annealed sample.

Figure 3 gives the temperature dependence of resistivity with warming and cooling for the as-prepared (sample A), 800 °C annealed (sample C), and 850 °C annealed (sample D) samples, respectively. A hysteresis is clearly observed around 130 K for all three samples, and this hysteresis is consistent with the first-order charge ordering phase transition. Even for the shoulder at 175 K, a small hysteresis is present.

Shown in Fig. 4 is the temperature dependence of ac susceptibility for the as-prepared (sample A), 600 °C annealed (sample B), 800 °C annealed (sample C), and 850 °C an-
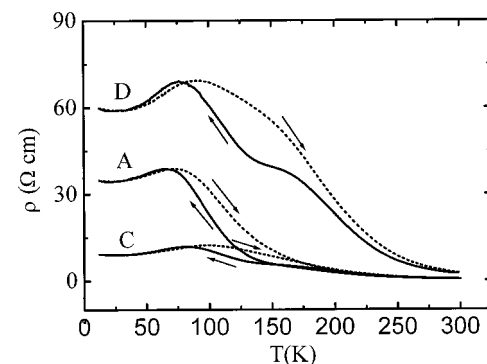
FIG. 3. Temperature dependence of resistivity with warming and cooling for the as-prepared (sample A), 800 °C annealed (sample C), and 850 °C annealed (sample D) samples, respectively.
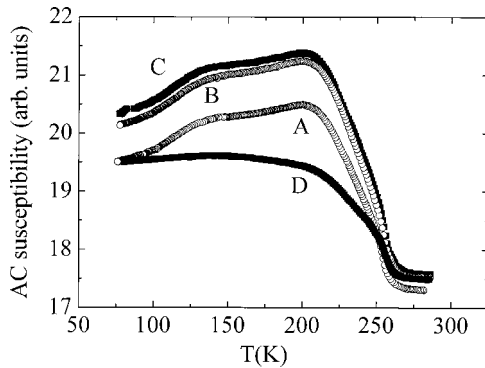
FIG. 4. Temperature dependence of ac susceptibility for the as-prepared (sample A), 600 °C annealed (sample B), 800 °C annealed (sample C), and 850 °C (sample D) samples, respectively.

nealed (sample D) samples, respectively. It shows the FM transition around 225 K and the charge ordering AFM transition around 130 K. Below 800 °C, the amplitude of the FM transition increases with the increase in the annealing temperature, while the drop of ac susceptibility, which is related to the AFM transition, does not change. Surprisingly, both the FM and AFM transition temperatures remain unchanged. For the 850 °C annealed sample, the amplitude of the FM transition is smaller than that of the as-prepared sample, although T_c remains the same, while the drop of ac susceptibility related to the AFM transition disappears. It should be pointed out that charge ordering transition exists in the 850 °C annealed sample as shown in the resistivity data. The absence of AFM transition and the presence of charge ordering in the 850 °C annealed sample may indicate that AFM transition and charge ordering do not necessarily occur simultaneously. We also got a sample with $y = 0.17$. This sample shows insulator-metal transition and paramagnetic-ferromagnetic transition at around 167 K as shown in Fig. 5. This result implies that $La_{0.5}Ca_{0.5}MnO_{3-y}$ samples can be driven into the CMR region by tuning their oxygen contents.

In order to further check the magnetic property of the 850 °C annealed sample, the temperature dependence of magnetization was measured using a SQUID magnetometer. Both zero-field-cooling (ZFC) and field-cooling (FC) data were recorded. Figures 6(a) and (b) show the temperature dependence of magnetization for the 850 °C annealed sample (sample D) with different magnetic fields. The ZFC curve
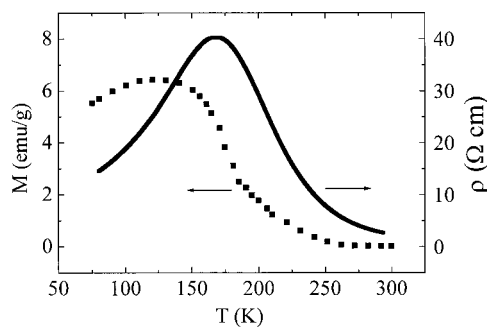
FIG. 5. Temperature dependence of resistivity and magnetization for sample with $y = 0.17$.
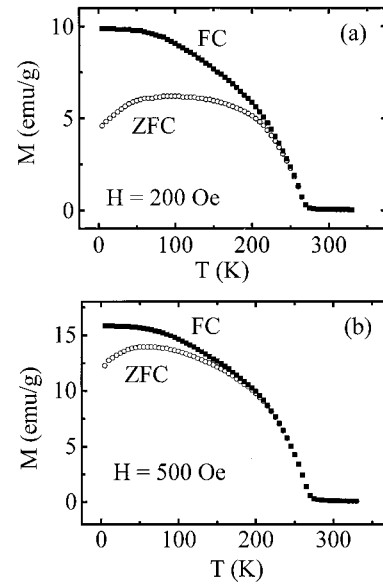
FIG. 6. Temperature dependence of magnetization for the 850 °C (sample D) annealed sample with different magnetic fields.

measured under 200 Oe shows a very broad peak. This peak shifts to lower temperature for the ZFC curve measured with 500 Oe, and becomes less prominent. It is also noted that the ZFC and FC curves show a large difference for the data obtained under 200 Oe, and this difference decreases for the ZFC and FC curves obtained under 500 Oe. The irreversible temperature, defined as the temperature at which the ZFC and FC curves begin to separate, also decreases from 239 to 202 K. The behavior is similar to that of a canted AFM or a cluster glass, which can be described as ferromagnetic clusters embedded in a spin-glass matrix. Oxygen vacancies in the structure could produce competing magnetic interactions as well as ferromagnetic clusters, making the sample magnetically disordered.

In order to show that the effect of annealing on the electrical transport and magnetic properties is really due to the reduction of oxygen content rather than the thermal effect, we also annealed the samples in flowing oxygen without graphite powder nearby. Figure 7 shows the temperature dependence of resistivity for the as-prepared sample, and the sample annealed at 850 °C in flowing O_2 for 12 h. The inset shows the temperature dependence of ac susceptibility for the two samples. The results suggest that annealing in flowing oxygen does not change the electrical transport and magnetic properties of $La_{0.5}Ca_{0.5}MnO_{3-y}$, in contrast to the results on samples annealed in flowing nitrogen with graphite nearby. Therefore it can be concluded that the variation of the electrical transport and magnetic properties of $La_{0.5}Ca_{0.5}MnO_{3-y}$ annealed in flowing nitrogen with graphite nearby is caused by the reduction of oxygen content in the samples.

Currently, evidences about inhomogeneity in both the CMR and the charge ordered samples are accumulating.[14,23,34–36] Pairing of charge ordering stripes in (La,Ca)MnO$_3$ was reported by Mori et al.[14] It was shown that pairs of Mn^{3+}O$_6$ stripe with associated large lattice con-
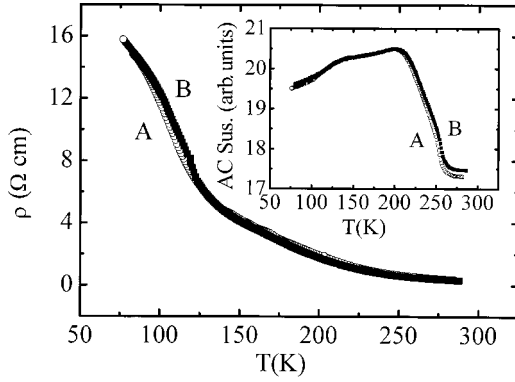
FIG. 7. Temperature dependence of resistivity for the as-prepared sample and the sample annealed at 850 °C in flowing O_2. The inset shows the temperature dependence of ac susceptibility for the two samples.

TABLE I. Resistivity at 280 and 100 K, and $\rho(100\ \text{K})/\rho(280\ \text{K})$, for different samples.

Sample	$\rho(100\ \text{K})/\rho(280\ \text{K})$	$\rho(280\ \text{K})$ (Ω cm)	$\rho(100\ \text{K})$ (Ω cm)
A	29	0.399	11.749
B	25	0.312	7.800
C	16	0.307	4.896
D	17	4.800	80.410

tractions due to the Jahn-Teller effect were separated periodically by stripes of nondistorted $Mn^{4+}O_6$ octahedra. The periodicity adopts integer values between two and five times the lattice parameter of the orthorhombic unit cell, corresponding to the commensurate doping levels with $x = \frac{1}{2}$, $\frac{2}{3}$, $\frac{3}{4}$, and $\frac{4}{5}$. Mori *et al.* also got the coherence lengths of the charge ordering stripes for $La_{1-x}Ca_xMnO_3$ with different x. Moreover, small regions without charge ordering were also found in the samples[10] and these regions may be related to the ferromagnetic metallic clusters. Uehara *et al.*[34] systematically studied the $La_{5/8-z}Pr_zCa_{3/8}MnO_3$ compounds and the results show that these compounds are electronically phase separated into submicrometer-scale mixture of insulating regions (with a particular type of charge ordering) and metallic, ferromagnetic domains. Very recently, it was shown that the CMR effect can also be explained by the phase separation model.[37] Levy *et al.* studied the electrical transport and magnetic properties of $La_{0.5}Ca_{0.5}MnO_3$ with different grain sizes, and the results show that the fraction of the ferromagnetic phase gradually decreases as the grain size increases, while the amount of the antiferromagnetic charge ordered phase increases.[25] The results are explained in terms of the influence of the defective structure at the grain surfaces on the phase separation, because the defective structure at the grain surfaces results in the formation of the ferromagnetic phase, and the effect is gradually removed with increasing grain size.

The results of our present work can be summarized as follows. The resistivity of the $La_{0.5}Ca_{0.5}MnO_{3-y}$ samples with small reduction of oxygen content decreases with the increase of the annealing temperature, however, the charge ordering temperature remains unchanged. While the ferromagnetic signal in the ac susceptibility measurements increases with the increase of the annealing temperature, the temperatures of FM and AFM transitions remain unchanged. In contrast, the resistivity of the samples with further reduction of oxygen content increases dramatically compared to that of the as-prepared sample, and the charge ordering temperature remains unchanged. Correspondingly, the ferromagnetic signal in the ac susceptibility measurement decreases, although the FM transition temperature does not change. For

sample with $y = 0.17$, insulator-metal and paramagnetic-ferromagnetic transitions occur at around 167 K. Moreover, the AFM transition disappears. These results can be understood more naturally in terms of the phase-separation model. For the as-prepared sample, both the FM phase and the CO AFM phase are present. The former is more conductive than the latter. Annealing below 800 °C results in a small amount of oxygen content reduction, as shown by the titration measurements. Oxygen content reduction has two effects. One is decreasing the ratio of Mn^{4+}/Mn^{3+} to drive the system to the CMR region, since $La_{0.5}Ca_{0.5}MnO$ is the phase boundary compound. Another effect is to introduce oxygen vacancies in the Mn-O network, which is important for conduction, and results in the local distortions in the structure. The oxygen content reduction destroys some part of the CO AFM regions. As a result the fraction of the FM regions increases, leading to the decrease of resistivity, and the increase of the FM regions for the samples. For the sample with $y = 0.17$, insulator-metal and paramagnetic-ferromagnetic transitions occur. For the sample with $y = 0.215$, the dramatic reduction of oxygen content induces strong distortion in the structure of the sample. As a result, the AFM transition is suppressed, and the FM magnetic structure changes to canted AFM or spin glass. It is noticed that for the samples annealed above 800 °C, the AFM transition is suppressed, however, the CO state still exists. Therefore the system becomes charge ordered and spin disordered. This implies that the AFM and charge ordered states may not necessarily occur concurrently.

It has been shown that oxygen content reduction has a similar effect on the electrical and magnetic properties as the decrease of Mn^{4+}/Mn^{3+} ratio via decreasing the Ca doping x in $La_{1-x}Ca_xMnO_3$ for $x < 0.33$.[38] Very recently, we showed that the electrical resistivity of $La_{0.4}Ca_{0.6}MnO_{3-y}$ increases upon oxygen content reduction.[39] In the present work, the resistivity of $La_{0.5}Ca_{0.5}MnO_{3-y}$ first decreases with oxygen content reduction, and then increases dramatically with further oxygen content reduction. Therefore it seems that the effect of the oxygen content variation on the properties of $La_{1-x}Ca_xMnO_{3-y}$ really depends on the Ca doping x or Mn^{4+}/Mn^{3+} ratio before oxygen reduction, and the behavior can be quite different for different Ca doping. The resistivity for the polycrystalline samples is determined by two contributions, i.e., contribution from the intragrain regions, and the contribution from the intergrain regions (grain boundaries). The effect of oxygen reduction may first occur around the grain boundaries and the surface layer of the grains. Further reduction extends the effect to the inner part of the grains. Table I shows the resistivity at 280 and 100 K, and $\rho(100\ \text{K})/\rho(280\ \text{K})$ for $La_{0.5}Ca_{0.5}MnO_{3-y}$ samples (A, B, C, and D

as defined in Fig. 2) with different oxygen contents. From sample A to sample C, both the resistivity and the resistivity ratio $\rho(100\text{ K})/\rho(280\text{ K})$ decrease, which indicates that the electrical transport property of the percolation route of the current changes upon oxygen reduction. While from sample C to sample D, the resistivity increases, but the resistivity ratio $\rho(100\text{ K})/\rho(280\text{ K})$ remains unchanged, this suggests that the electrical transport property of the percolation routes of the current does not change, however, the amount of the conductive phase or routes decreases. Thus the reduction of oxygen content changes the coexistence of the conductive FM phase and the insulating charge ordered AFM phase. It should be mentioned that for sample D ($La_{0.5}Ca_{0.5}MnO_{2.785}$), the ratio of $Mn^{3+}/(Mn^{4+}+Mn^{3+})$ is close to 93%, which is comparable to that of $La_{0.93}Ca_{0.07}MnO_3$. However, $La_{0.93}Ca_{0.07}MnO_3$ should be a ferromagnetic insulator according to the phase diagram with T_c about 125 K, charge ordering temperature T_{c0} about 60 K, and $\rho(100\text{ K})/\rho(300\text{ K})$ larger than 900.[40] These property features are quite different from those of sample D, whose Mn^{3+}/Mn^{4+} ratio is comparable to that of $La_{0.93}Ca_{0.07}MnO_3$. For $La_{0.5}Ca_{0.5}MnO_{2.83}$, the ratio of $Mn^{3+}/(Mn^{4+}+Mn^{3+})$ is close to 84%, comparable to that of $La_{0.84}Ca_{0.16}MnO_3$. However, $La_{0.84}Ca_{0.16}MnO_3$ is a ferromagnetic insulator, in contrast to the electrical transport and magnetic properties of $La_{0.5}Ca_{0.5}MnO_{2.83}$, which shows insulator-metal transition and paramagnetic-ferromagnetic transition around 167 K.

This clearly shows that besides the Mn^{3+}/Mn^{4+} ratio, other factors, such as the electron-phonon interaction and spin interaction are also important in the control of the various properties of manganites. It should be pointed out that a different phase diagram can be obtained for $La_{1-x}Ca_xMnO_{3-y}$ with less oxygen content if one anneals $La_{1-x}Ca_xMnO_{3-y}$ at a certain temperature in flowing N_2 with graphite powder nearby.

In summary, we have studied the electrical transport and magnetic properties of $La_{0.5}Ca_{0.5}MnO_{3-y}$ with different oxygen contents. The resistivity of the samples decreases with small reduction of oxygen content, while the magnetic property does not show obvious change. Further reduction of oxygen content leads to a dramatic increase in resistivity, decrease in the amplitude of the ferromagnetic transition at 225 K, and the disappearance of antiferromagnetic transition at 130 K. Insulator-metal transition and paramagnetic-ferromagnetic transition occur around 167 K for the sample with $y = 0.17$. The results are explained in terms of the effect of oxygen content on the coexistence of FM metallic and charge ordered insulating AFM phases.

*E-mail address: ygzhao@tsinghua.edu.cn

[1] S. Chahara, T. Ohno, K. Kasai, and Y. Kozono, Appl. Phys. Lett. **63**, 1990 (1993).

[2] R. von Helmolt, J. Wecker, B. Holzapfel, L. Schultz, and K. Samwer, Phys. Rev. Lett. **71**, 2331 (1993).

[3] S. Jin, T. H. Tiefel, M. McCormack, R. A. Fastnacht, R. Ramesh, and L. H. Chen, Science **264**, 413 (1994).

[4] C. Zener, Phys. Rev. **82**, 403 (1951); P. W. Anderson and H. Hasegawa, *ibid.* **100**, 675 (1955); P. G. de Gennes, *ibid.* **118**, 141 (1960).

[5] A. J. Millis, P. B. Littlewood, and B. I. Shraiman, Phys. Rev. Lett. **74**, 5144 (1995); **77**, 175 (1996).

[6] T. T. M. Palstra, A. P. Ramirez, S. W. Cheong, B. R. Zegarski, P. Schiffer, and J. Zaanen, Phys. Rev. B **56**, 5104 (1997).

[7] G. M. Zhao, K. Conder, H. Keller, and K. A. Muller, Nature (London) **381**, 676 (1996).

[8] P. E. Schiffer, A. P. Ramirez, W. Bao, and S. W. Cheong, Phys. Rev. Lett. **75**, 3336 (1995).

[9] C. H. Chen and S-W. Cheong, Phys. Rev. Lett. **76**, 4042 (1996).

[10] P. G. Radaelli, D. E. Cox, M. Marezio, and S-W Cheong, Phys. Rev. B **55**, 3015 (1997).

[11] G. Papavassiliou, M. Fardis, F. Milia, A. Simopoulos, G. Kallias, M. Pissas, D. Niarchos, N. Ioannidis, C. Dimitropoulos, and J. Dolinsek, Phys. Rev. B **55**, 15 000 (1997).

[12] A. Sundaresan, P. L. Paulose, R. Mallik, and E. V. Sampathkumaran, Phys. Rev. B **57**, 2690 (1998).

[13] S. Mori, C. H. Chen, and S-W. Cheong, Phys. Rev. Lett. **81**, 3972 (1998).

[14] S. Mori, C. H. Chen, and S-W Cheong, Nature (London) **392**, 473 (1998).

[15] G. Allodi, R. De Renzi, F. Licci, and M. W. Pieper, Phys. Rev. Lett. **81**, 4736 (1998).

[16] J. M. Gonzalez-Galbet, E. Herrero, N. Rangavittal, J. M. Alonso, J. L. Martinez, and M. Vallet-Regi, J. Solid State Chem. **148**, 158 (1999).

[17] G. Kallias, M. Pissas, E. Devlin, A. Simopoulos, and D. Niarchos, Phys. Rev. B **59**, 1272 (1999).

[18] Y. Yoshinari, P. C. Hammel, J. D. Thompson, and S-W Cheong, Phys. Rev. B **60**, 9275 (1999).

[19] Ruiping Wang, Rajappan Mahesh, and Mitsuru Itoh, Phys. Rev. B **60**, 14 513 (1999).

[20] Joonghoe Dho, Ilryong Kim, and Soonchil Lee, Phys. Rev. B **60**, 14 545 (1999).

[21] C. H. Chen, S. Mori, and S-W Cheong, Phys. Rev. Lett. **83**, 4792 (1999).

[22] G. Papavassiliou, M. Fardis, M. Belesi, T. G. Maris, G. Kallias, M. Pissas, D. Niarchos, C. Dimitropoulos, and J. Dolinsek, Phys. Rev. Lett. **84**, 761 (2000).

[23] Q. Huang, J. W. Lynn, R. W. Erwin, A. Santoro, D. C. Dender, V. N. Smolyaninova, K. Ghosh, and R. L. Greene, Phys. Rev. B **61**, 8895 (2000).

[24] V. N. Smolyaninova, Amlan Biswas, X. Zhang, K. H. Kim, Bog-Gi Kim, S-W. Cheong, and R. L. Greene, Phys. Rev. B **62**, R6093 (2000).

[25] P. Levy, F. Parisi, G. Polla, D. Vega, G. Leyva, H. Lanza, R. S. Freitas, and L. Ghivelder, Phys. Rev. B **62**, 6437 (2000).

[26] A. Simopoulos, G. Kallias, E. Devlin, and M. Pissas, Phys. Rev. B **63**, 054403 (2000).

[27] A. P. Ramirez, P. Schiffer, S-W. Cheong, C. H. Chen, W. Bao, T. T. M. Palstra, B. Zegarski, P. L. Gammel, and D. J. Bishop, Phys. Rev. Lett. **76**, 3188 (1996).

[28] H. Kuwahara, Y. Tomioka, A. Asamitsu, Y. Moritomo, and Y. Tokura, Science **270**, 961 (1995).

[29] Y. Tomioka, A. Asamitsu, Y. Moritomo, H. Kuwahara, and Y. Tokura, Phys. Rev. Lett. **74**, 5108 (1995).

[30] V. Kiryukhin, D. Casa, J. P. Hill, B. Keimer, A. Vigliante, Y. Tomioka, and Y. Tokura, Nature (London) **386**, 813 (1997).

[31] A. Barnabe, A. Maignan, M. Hervieu, F. Damay, C. Martin, and B. Raveau, Appl. Phys. Lett. **71**, 3907 (1997).

[32] F. Damay, C. Martin, A. Maignan, M. Hervieu, B. Ravieu, F. Bouree, and G. Andre, Appl. Phys. Lett. **73**, 3772 (1998).

[33] E. Bloom, Jr., T. Y. Kometani, and J. W. Mitchell, J. Inorg. Nucl. Chem. **40**, 403 (1978).

[34] M. Uehara, S. Mori, C. H. Chen, and S. W. Cheong, Nature (London) **399**, 560 (1999).

[35] M. Fath, S. Freisen, A. A. Menovsky, Y. Tomioka, J. Aarts, and J. A. Mydosh, Science **285**, 1540 (1999).

[36] R. D. Merithew, M. B. Weissman, F. M. Hess, P. Sporadling, E. R. Nowak, J. O'Donnell, J. N. Eckstein, Y. Tokura, and Y. Tomioka, Phys. Rev. Lett. **84**, 3442 (2000).

[37] Matthias Mayr, Adriana Moreo, Jose A. Verges, Jeanette Arispe, Adrian Feiguin, and Elbio Dagotto, Phys. Rev. Lett. **86**, 135 (2001).

[38] H. L. Ju, J. Gopalakrishnan, J. L. Peng, Q. Li, G. C. Xiong, T. Venkatesan, and R. L. Greene, Phys. Rev. B **51**, 6143 (1995).

[39] W. Cai, Y. G. Zhao, Y. Z. He, L. W. Zhang, M. H. Zhu, H. S. Huang, M. L. Liu, and B. S. Cao, Phys. Status Solidi A **187**, 529 (2001).

[40] S. W. Cheong and H. Y. Huang, in *Contribution to Colossal Magnetoresistance Oxides*, edited by Y. Tokura Monographs in Condensed Matter Science (Gordon & Breach, London, 2000).